BBA - Molecular Cell Research 1868 (2021) 119113

Contents lists available at ScienceDirect

BBA - Molecular Cell Research

journal homepage: www.elsevier.com/locate/bbamcr

Competitive binding of extracellular accumulated heparan sulfate reduces lysosomal storage defects and triggers neuronal differentiation in a model of Mucopolysaccharidosis IIIB

Valeria De Pasquale [b], Gianluca Scerra [a], Melania Scarcella [a], Massimo D'Agostino [a,*], Luigi Michele Pavone [a,*]

[a] Department of Molecular Medicine and Medical Biotechnology, University of Naples Federico II, Via S. Pansini 5, 80131 Naples, Italy
[b] Department of Veterinary Medicine and Animal Productions, University of Naples Federico II, Via F. Delpino 1, 80127 Naples, Italy

ARTICLE INFO

Keywords:
Mucopolysaccharidosis
NAGLU
Heparan sulfate
SK-NBE
Neuronal differentiation

ABSTRACT

Mucopolysaccharidoses (MPSs) are a group of inherited lysosomal storage disorders associated with the deficiency of lysosomal enzymes involved in glycosaminoglycan (GAG) degradation. The resulting cellular accumulation of GAGs is responsible for widespread tissue and organ dysfunctions. The MPS III, caused by mutations in the genes responsible for the degradation of heparan sulfate (HS), includes four subtypes (A, B, C, and D) that present significant neurological manifestations such as progressive cognitive decline and behavioral disorders. The established treatments for the MPS III do not cure the disease but only ameliorate non-neurological clinical symptoms. We previously demonstrated that the natural variant of the hepatocyte growth factor NK1 reduces the lysosomal pathology and reactivates impaired growth factor signaling in fibroblasts from MPS IIIB patients. Here, we show that the recombinant NK1 is effective in rescuing the morphological and functional dysfunctions of lysosomes in a neuronal cellular model of the MPS IIIB. More importantly, NK1 treatment is able to stimulate neuronal differentiation of neuroblastoma SK-NBE cells stable silenced for the NAGLU gene causative of the MPS IIIB. These results provide the basis for the development of a novel approach to possibly correct the neurological phenotypes of the MPS IIIB as well as of other MPSs characterized by the accumulation of HS and progressive neurodegeneration.

1. Introduction

Mucopolysaccharidoses (MPSs) are lysosomal storage diseases (LSDs) due to inherited deficiencies of lysosomal enzymes required for the breakdown of glycosaminoglycans (GAGs) [1]. The lack of GAG degradation leads to tissue damages and organ dysfunctions accounting for MPS clinical manifestations such as neurological disorders, heart disease, skeletal and joint abnormalities, respiratory problems, coarse facial features, hearing loss, corneal clouding, and others. As GAGs are a heterogeneous group of high sulfated linear polysaccharides, which include chondroitin sulfate (CS), dermatan sulfate (DS), heparan sulfate (HS), and keratan sulfate (KS), depending on the specific GAG build-up due to the missing or malfunctioning enzyme, MPSs are categorized into seven types (I, II, III, IV, VI, VII and IX) which differ in their incidence, clinical complications, and degree of severity [2]. Some MPS types are further classified into subtypes such as in the case of the MPS III, also known as Sanfilippo syndrome, caused by mutations in genes responsible for the degradation of HS [1].

There are four distinct MPS III subtypes, namely A, B, C, and D, which differ in the mutated gene and the consequent lack of the enzyme. The main clinical manifestation of the MPS III, regardless of the subtype, is a progressive degeneration of the central nervous system (CNS) leading to mental retardation, hyperactivity, aggressive behavior, and sleep disturbances, together with variable mild somatic symptoms [1,3,4]. The age of the onset and severity of the clinical symptoms may differ among the different MPS III subtypes, but most patients usually die in the second or third decade of their life, and only in rare and attenuated cases they can survive to the fourth decade. Currently, there is no effective therapy for the treatment of the neurological symptoms of any MPS III subtype.

Recently, we focused much effort on a better characterization of the molecular mechanisms underlying HS storage defects at the cellular

* Corresponding authors.
E-mail addresses: massimo.dagostino@unina.it (M. D'Agostino), luigimichele.pavone@unina.it (L.M. Pavone).

https://doi.org/10.1016/j.bbamcr.2021.119113
Received 2 April 2021; Received in revised form 19 July 2021; Accepted 23 July 2021
Available online 28 July 2021
0167-4889/© 2021 The Authors. Published by Elsevier B.V. This is an open access article under the CC BY license (http://creativecommons.org/licenses/by/4.0/).

level in MPS IIIB disease with the final goal to develop and assess a novel therapeutic approach for the treatment of such devastating disease [5–10]. The MPS IIIB subtype is an autosomal recessive disorder caused by the deficiency of the α-*N*-acetylglucosaminidase (NAGLU) enzyme involved in the HS degradation pathway. Since multiple evidence showed that, in MPS diseases, GAG storage is not restricted to the lysosomal compartment, but it is also redistributed to different cellular and extracellular localizations [11–19], we demonstrated that the extracellular accumulation of HS contributes to the MPS IIIB phenotypes by interfering with growth factor-induced receptor activation and downstream signaling [7,20]. On the basis of this pathogenic mechanism, we developed an innovative therapeutic strategy able to restore signaling pathways disrupted in the disease [7]. The novel therapeutic approach for the MPS IIIB is based on the use of a recombinant natural spliced variant of the hepatocyte growth factor, namely NK1, able to bind with high affinity the extracellular accumulated HS, thus reestablishing the physiological equilibrium between endogenous ligands, HS, and receptors, which underlies the normal cellular activities [21].

In this work, we generated a cellular model of the MPS IIIB neuronal phenotype by silencing NAGLU gene expression in the human neuroblastoma cell line SK-NBE [22], in order to assess the ability of the recombinant NK1 to rescue the lysosomal defects in this MPS IIIB disease model. SK-NBE cultured cells, upon retinoic acid (RA) exposure and serum deprivation, undergo to differentiation process showing a typical neuronal phenotype demonstrated by neurite extensions, thus representing a valuable cell model system for studying disease neurophysiopathology [23,24]. These cells, previously silenced for NAGLU, recapitulate the lysosomal phenotype of the MPS IIIB and are unable to differentiate into neurons, thus providing us a useful tool for testing *in vitro* the therapeutic effect of the recombinant NK1.

2. Results and discussion

2.1. NAGLU-silenced neuroblastoma SK-NBE recapitulates the MPS IIIB lysosomal defects

In order to investigate the effects of NK1 treatment on lysosomal dysfunctions in a neuronal model of the MPS IIIB disease, we generated two stable clones differentially silenced for NAGLU, the causative gene of the disease. As previously done by us [6], we used a pool of three different shRNA directed against the human NAGLU mRNA in order to silence the expression of the NAGLU gene in the human neuroblastoma SK-NBE cell line. These cells are able to differentiate into neuron-like cells, thus serving as a good model to study *in vitro* the neuronal defects caused by NAGLU silencing and consequent lysosomal impairment. After the screening of the silenced clones, by measuring NAGLU enzymatic activity, we selected two clones: clone 5 (cl 5) almost completely deprived of the NAGLU activity, and clone 8 (cl 8) with a residual enzymatic activity (Fig. 1A). Notably, clone 5 showed almost the same residual NAGLU enzymatic activity of the MPS IIIB fibroblasts, while adult human dermal fibroblasts (HDFa) from a healthy subject, used as an internal positive control, showed a high NAGLU enzymatic activity. Moreover, we selected a pool of stable clones transfected with a non-targeting shRNA (CTRL) as a control for further experiments.

In order to evaluate the correlation between the residual enzymatic activity of the clones and NAGLU protein levels, we performed a Western blotting analysis. The results obtained demonstrated the absence of the protein in clone 5, and a significant reduction of NAGLU protein levels in clone 8 compared to that of CTRL clone (Fig. 1B). These findings were consistent with the NAGLU enzymatic activity of the two clones. Indeed, the reduction of NAGLU protein levels resulted in about 80% and 95% reduction of NAGLU catalytic activity in the SK-NBE shNAGLU clone 8 and clone 5, respectively, as compared to that of the SK-NBE CTRL clone.

Then, we evaluated whether the two NAGLU silenced clones would recapitulate the lysosomal defects seen in the cells from MPS IIIB patients. Although to different extents, both clones 5 and 8 showed an accumulation of enlarged lysosomes (Fig. 2) as detected by the Lamp1-positive structures revealed by immunostaining (Fig. 2, left panels) and confirmed by the LysoTracker staining (Fig. 2, right panels).

Since the lysosomal enlargement in MPS diseases leads to the accumulation of HS on the cell membrane which in turn inactivates a plethora of cell signaling [14,20,25,26], we investigated whether HS accumulates on the cell membrane of the SK-NBE stable clones. As detected by the specific HS antibody 10-E4, both clones 5 and 8 showed a positive 10E4 staining on the cell membrane (Supplementary Fig. S1). This is a confirmation of the HS build-up on the cell membrane of the SK-NBE NAGLU silenced clones consequent to the impairment of lysosomal functions due to the absence of the NAGLU enzyme. The 10E4 epitope lies in the *N*-sulfated regions of the HS chain, therefore the accumulation of HS, in the SK-NBE NAGLU silenced clones, is observed at the cell surface and not in the lysosomal compartments since this antibody recognizes membrane-tethered HS [27–30]. Indeed, we performed an immunofluorescence staining with the 10E4 antibody on the MPS I and MPS IIIB fibroblasts and HDFa control cells, and we obtained the same results further confirming the accumulation of HS on the cell membrane of the MPS diseased cells (Supplementary Fig. S2).

2.2. Fluorescence-conjugated lectin probe reveals GAGs/HS accumulation within the lysosomes

In order to study and reveal the intracellular GAGs/HS accumulation in our cellular model, we tested whether a fluorescent lectin from Triticum vulgaris (wheat) FITC conjugate (Lectin-FITC), able to recognize sugars or glycoproteins containing *N*-acetylglucosamine residues [31],

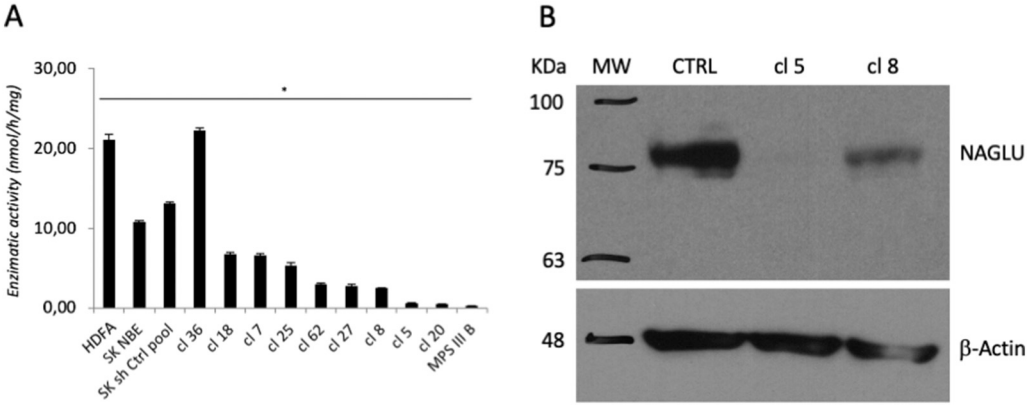

Fig. 1. NAGLU silencing in neuroblastoma SK-NBE cells. (A) NAGLU enzymatic activity in the extracts from SK-NBE CTRL and SK-NBE NAGLU silenced clones. Cell lysates from untransfected SK-NBE cells and transfected clones were assayed for NAGLU enzymatic activity, normalized for protein content, and compared to that of HDFa and MPS IIIB fibroblasts, used as controls. Asterisks indicate the statistically significant differences: (*) p-value < 0.05 (B) NAGLU protein levels in SK-NBE CTRL and SK-NBE NAGLU silenced clones (cl 5 and cl 8) as measured by Western blotting analysis. To monitor equal loading of the proteins in the gel lanes, the blot was re-probed using an anti-β-actin antibody.

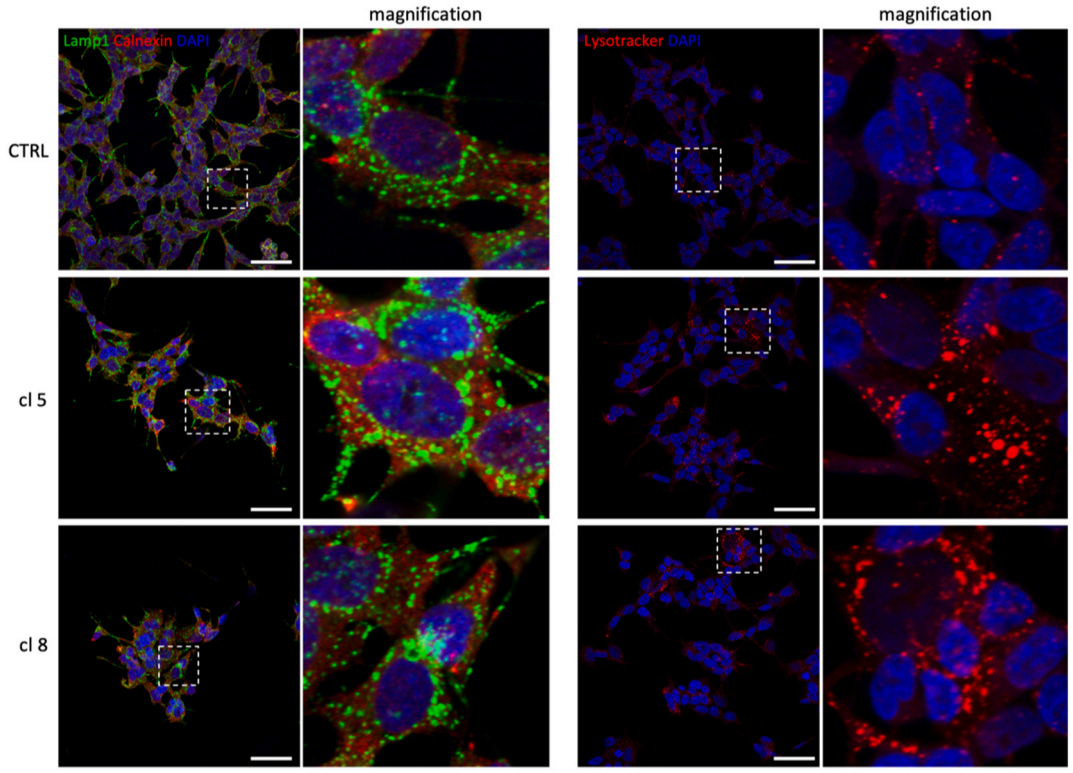

Fig. 2. NAGLU silenced stable clones 5 and 8 showed an accumulation of enlarged lysosomes as detected by both Lamp1 immunostaining and LysoTracker staining. SK-NBE CTRL clone and NAGLU silenced stable clones (cl 5 and cl 8) were seeded on coverslips and processed for indirect immunofluorescence after 24 h by using specific antibodies against Calnexin (ER marker), Lamp1 or LysoTracker (Lysosomal markers), and DAPI (Nuclear marker). Magnifications are relative to the dashed white squares. Single focal sections are shown. Scale bar: 50 μm.

would allow us to detect the intracellular accumulation of undegraded or partially degraded HS within the enlarged lysosomes of the selected NAGLU silenced clones.

The double staining with the lysosomal marker Lamp1 showed the colocalization of the Lectin-FITC with Lamp1 revealing the accumulation at the lysosomal compartment of undegraded HS, and/or of other sugars or glycoproteins containing *N*-acetylglucosamine residues (Supplementary Fig. S3). Indeed, we performed a double staining with the LysoTracker probe and Lectin-FITC on the MPS I and MPS IIIB fibroblasts and HDFa control cells (Supplementary Fig. S4), and we obtained the same results observed in the SK-NBE stable clones, further confirming the accumulation of the HS within the lysosomes of the MPS diseased cells. Moreover, in the MPS IIIB derived fibroblasts, in addition to the lysosomal compartment stained by LysoTracker, the lectin labeling is also evident at the cell membrane.

Thus, in order to have a picture of the double accumulation of the HS both on the cell membrane and inside the lysosomes, which is at the base of our therapeutic approach, we performed a double staining with the 10E4 antibody that recognizes the extracellular HS and with the lectin that recognizes the undegraded HS within the lysosome (Fig. 3). Clones 5 and 8 showed a marked staining of both cell membrane and intracellular compartment, although the quantification of the HS positive cells revealed a major number of HS positive cells in clone 5 compared to clone 8, consistent with the different levels of NAGLU silencing in the two clones.

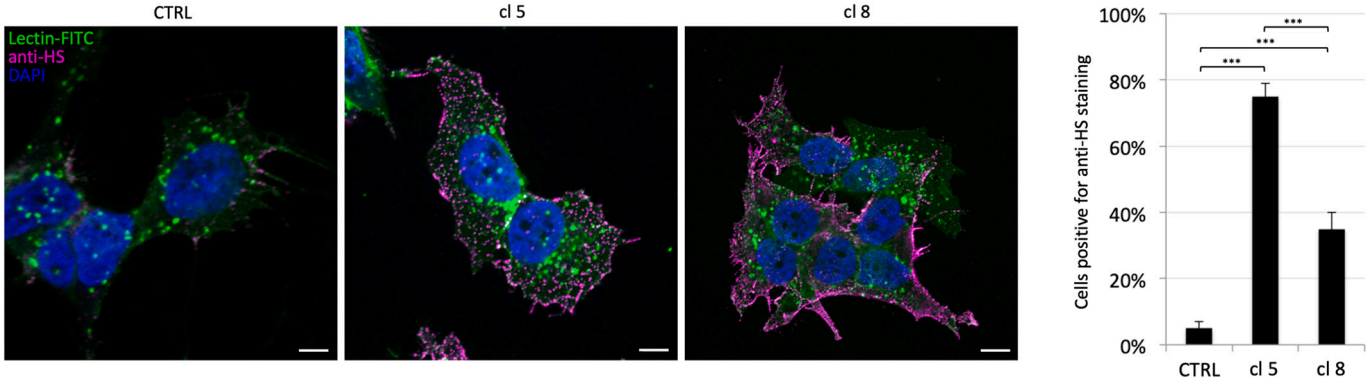

Fig. 3. Heparan sulfate (HS) accumulation in NAGLU silenced stable clones. SK-NBE CTRL clone and NAGLU silenced stable clones (cl 5 and cl 8) were seeded on coverslips and processed for indirect immunofluorescence after 24 h by using the fluorescent Lectin (GAG/HS marker), specific antibodies against HS. Nuclei were decorated by DAPI staining. Quantification analysis was made by using a sample of 200 cells from three independent experiments. Single focal sections are shown. Scale bar: 50 μm. Asterisks indicate the statistically significant differences: (***) p-value < 0.0001.

2.3. NK1 treatment reduces lysosomal defects in a neuronal cellular model of the MPS IIIB disease

Since our new fluorescence lectin probe is able to detect the intracellular accumulated GAGs/HS, we asked whether NK1 treatment would be able to reduce HS accumulation and lysosome morphology in NAGLU silenced neuroblastoma SK-NBE clones. However, given that the different classes of GAG chains are enzymatically polymerized in the Golgi apparatus, we also tested the selective effect of NK1 in reducing the lysosomal GAG accumulation in comparison to the Golgi population. As shown in Fig. 4, NK1 treatment did not affect the intracellular distribution of GAGs in the SK-NBE CTRL clone as revealed by the co-staining of the fluorescent lectin and GM130 (marker of the Golgi complex). Moreover, NAGLU silenced neuroblastoma clones showed an increased level of the GAGs/HS at the lysosomal compartment and a reduced one at the Golgi apparatus as revealed by the colocalization analysis of Lectin/Lamp1 and Lectin/GM130, respectively. Strikingly, NK1 treatment rescued the HS levels in both lysosomal and Golgi compartments indicating that NK1 is able to rescue the physiological GAGs/HS distribution within the cell together with a reduction of Lamp1 positivity. Indeed, NK1 treatment also rescued the HS accumulation on the plasma membrane.

2.4. NK1 treatment stimulates differentiation into neuron-like cells of the NAGLU silenced SK-NBE clones

SK-NBE neuroblastoma cells are able to differentiate into neurons under serum deprivation and retinoic acid (RA) treatment [23,24]. Thus, we tested whether NAGLU silencing would interfere with neuronal differentiation. We stained the differentiated clones with the neuronal marker β3-Tubulin, and, as it is shown in Fig. 5, clone 5 was unable to differentiate, while clone 8, which has a residual NAGLU activity, was still able to differentiate, in accordance with the fact that the severity of the phenotype in patients is strictly related to the residual enzymatic activity.

Overall, these results prompted us to explore the *in vitro* efficacy of NK1 in promoting the differentiation process in the MPS IIIB cellular model. Thus, we tested whether NK1 treatment would stimulate the differentiation of SK-NBE NAGLU silenced clone 5 by adding NK1 to the differentiation media. As it is shown in Fig. 6 (upper panels), NK1 was able to induce the differentiation into neuron-like cells also of the NAGLU silenced clone 5. Moreover, we stained the differentiated stable clones with Lamp1 (Fig. 6, lower panels), and found that in the undifferentiated clone 5 the lysosomes are trapped into the perinuclear region because clone 5 does not grow neurites, while in the differentiated ones the lysosomes populate the axons. Impaired axonal lysosome delivery was recently demonstrated to contribute to the pathogenesis also of other lysosomal storage diseases such as reported by Roney and

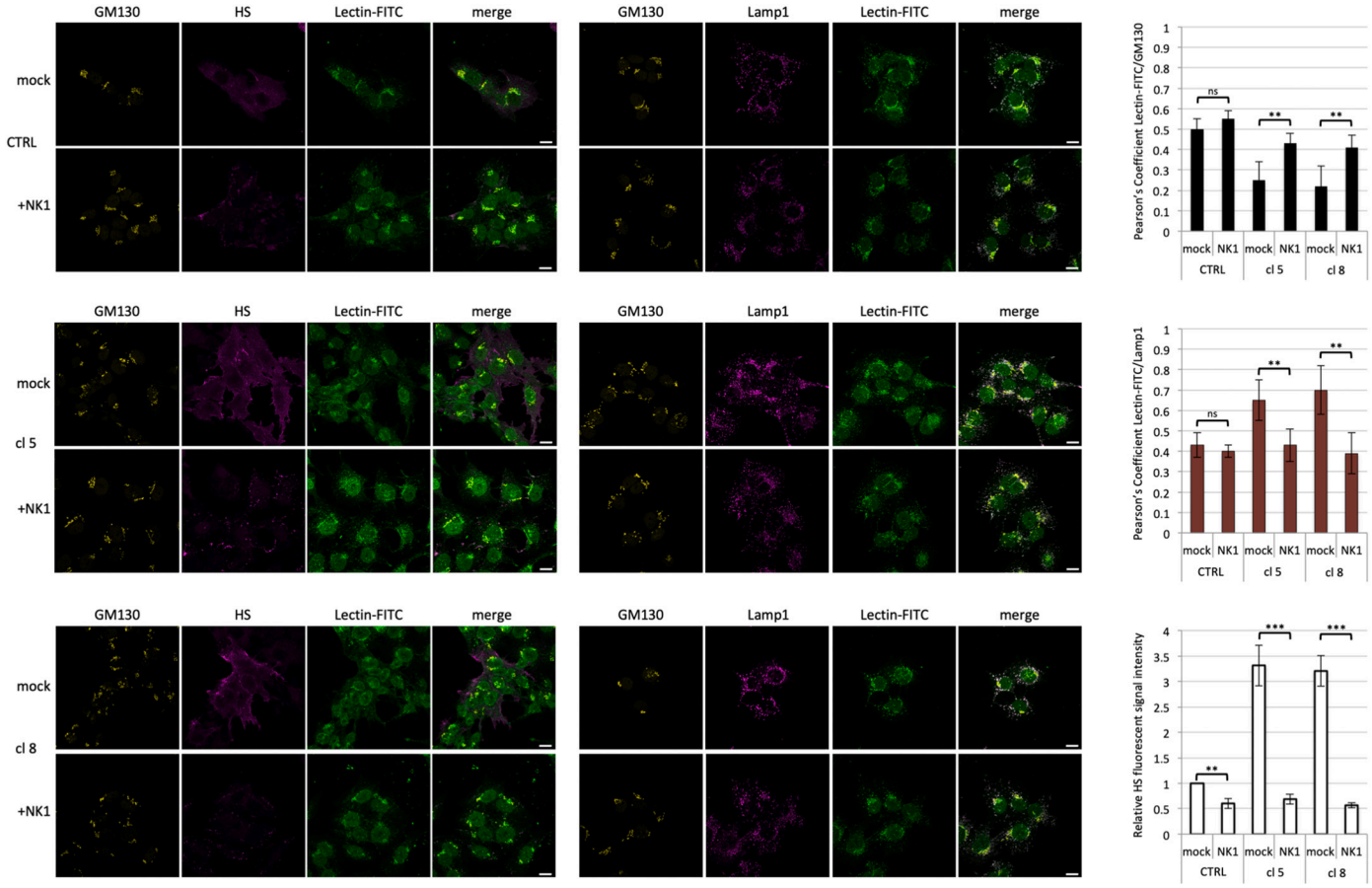

Fig. 4. NK1 treatment rescues GAGs/HS distribution in NAGLU silenced stable clones. SK-NBE CTRL clone and NAGLU silenced stable clones (cl 5 and cl 8) were seeded on coverslips and processed for indirect immunofluorescence after 48 h of NK1 treatment. The intracellular distribution of GAGs/HS (detected by using the Lectin-FITC probe) was assessed by colocalization analysis with Golgi and lysosomal markers (GM130 and Lamp1, respectively). The histograms on the right represent either the quantification of the colocalization between Lectin-FITC and GM130 (top), Lectin-FITC and Lamp1 (middle), or the mean fluorescence intensity of HS among the different experimental conditions (bottom). 50 randomly chosen cells from three independent experiments were used for quantifications. Single focal sections are shown. Scale bar: 50 μm. Asterisks indicate the statistically significant differences: (***) p-value < 0.0001, (**) p-value < 0.001, (ns) p-value not significant.

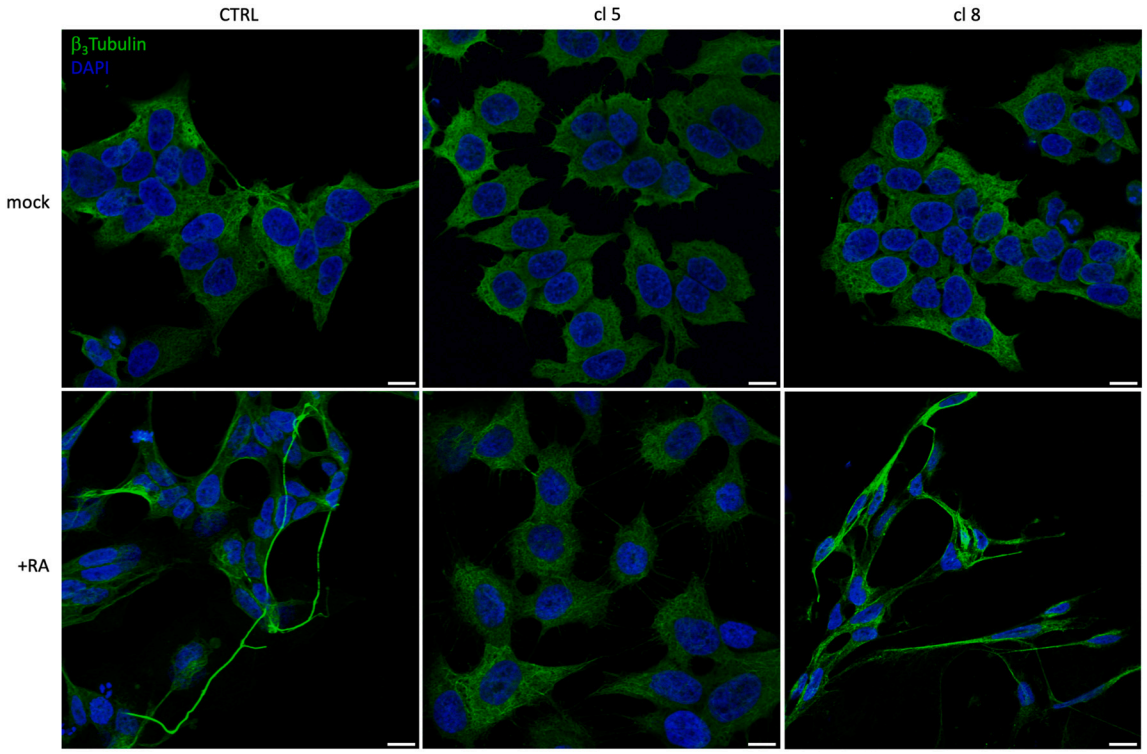

Fig. 5. Defect of neuronal differentiation of NAGLU silenced stable clone 5. SK-NBE CTRL clone and NAGLU silenced stable clones (cl 5 and cl 8) were seeded on coverslips and treated with 10 μM retinoic acid (RA) and 0,5% FBS for 3 weeks before being processed for indirect immunofluorescence by using a specific antibody against β_3-Tubulin. Nuclei were decorated by DAPI staining. Single focal sections are shown. Scale bar: 50 μm.

colleagues [32].

Finally, we tested the effect of NK1 treatment on HS accumulation in the differentiated NAGLU silenced clones. The results obtained showed that NK1 treatment significantly reduces HS build-up in both differentiated NAGLU silenced stable clones 5 and 8 (Fig. 7). Although further studies are needed to understand the correct intracellular signaling pathways activated by NK1, these results strongly suggest that NK1 treatment, with its action to bind and reduce the HS accumulated in the NAGLU-silenced neuroblastoma cells, is able to reactivate signals necessary for the neuronal differentiation process and generate undiseased neurons.

2.5. NK1 treatment stimulates lysosomal exocytosis in the NAGLU silenced SK-NBE clones

Since lysosomal exocytosis is impaired in most lysosomal storage diseases, as we have also recently shown for MPS diseased fibroblasts [33], we asked whether NK1 treatment would restore the normal organelle trafficking in our MPS IIIB cellular model. In MPS IIIB fibroblasts, pathologically enlarged lysosomes are retained within the endoplasmic reticulum (ER) membranes, thereby ultimately limiting their motility and secretion. The same effect is detectable in our SK-NBE NAGLU silenced clones when compared to the CTRL clone by using a β-hexosaminidase assay. As it is shown in Fig. 8 (upper left panel), the secretion of the β-hexosaminidase enzyme into the medium of the MPS IIIB clones is reduced in comparison with the CTRL clone, mirroring the severity of NAGLU silencing in our model. Upon NK1 treatment, in a time-dependent manner, the lysosomal secretion of the β-hexosaminidase is completely recovered after 36 h. These results explain for the first time that the mechanisms of action of NK1 in reducing the lysosomal defects in the MPS cellular model involve the reactivation of the physiological lysosomal exocytosis and secretion.

3. Conclusions

The major burden of MPS diseases is represented by the early-onset of severe progressive neurodegeneration [3,34–36]. Despite clinical trials with enzyme replacement therapy (ERT), substrate reduction therapy (SRT), and gene therapy are currently been conducted, no effective therapeutic option for MPS III patients is available today [37,38]. In the present work, we demonstrate the efficacy of a novel strategy for the treatment of the MPS III lysosomal defects using a neuronal cellular model of the MPS IIIB. This approach is based on the use of the recombinant NK1 protein, a natural spliced variant of HGF, which binds with high affinity the HS that accumulates on the cell surface and extracellular matrix of affected cells.

Extensive research over the past years has established that, in addition to the primary lysosomal accumulation of HS, dysregulation of multiple cellular processes such as cell signaling defects, impaired autophagy, neuroinflammation, and oxidative stress are involved in the MPS III neuropathological mechanisms [4,11,14,20,36,39,40]. Noticeably, the abnormal cellular pathways correlate not only with the accumulation of undigested HS in the lysosomes but also with an increase of HS oligosaccharides on the cell membrane and extracellular matrix [11–20]. In particular, in the central nervous system (CNS) of MPS I, II, III, and VII patients, secondary accumulation of HS and variable composition of HS proteoglycans (HSPGs) at non-lysosomal sites have been detected by post-mortem neuroimaging analyses [19]. Neurodevelopmental changes in excitatory synaptic structures and function resulted to be associated with enhanced expression levels of extracellular HS and the HSPG glypican 4 in the cerebral cortex of MPS IIIA mice [18]. In the MPS IIIB mouse brain, a differential distribution of HS glycoforms, with increased levels of extracellular HS and enhanced expression of HS biosynthetic enzymes and fibroblast growth factors (FGFs) has been reported [13].

The abnormal levels of extracellular HS and cell surface-tethered HS proteoglycans in the CNS of MPS patients have a detrimental role in

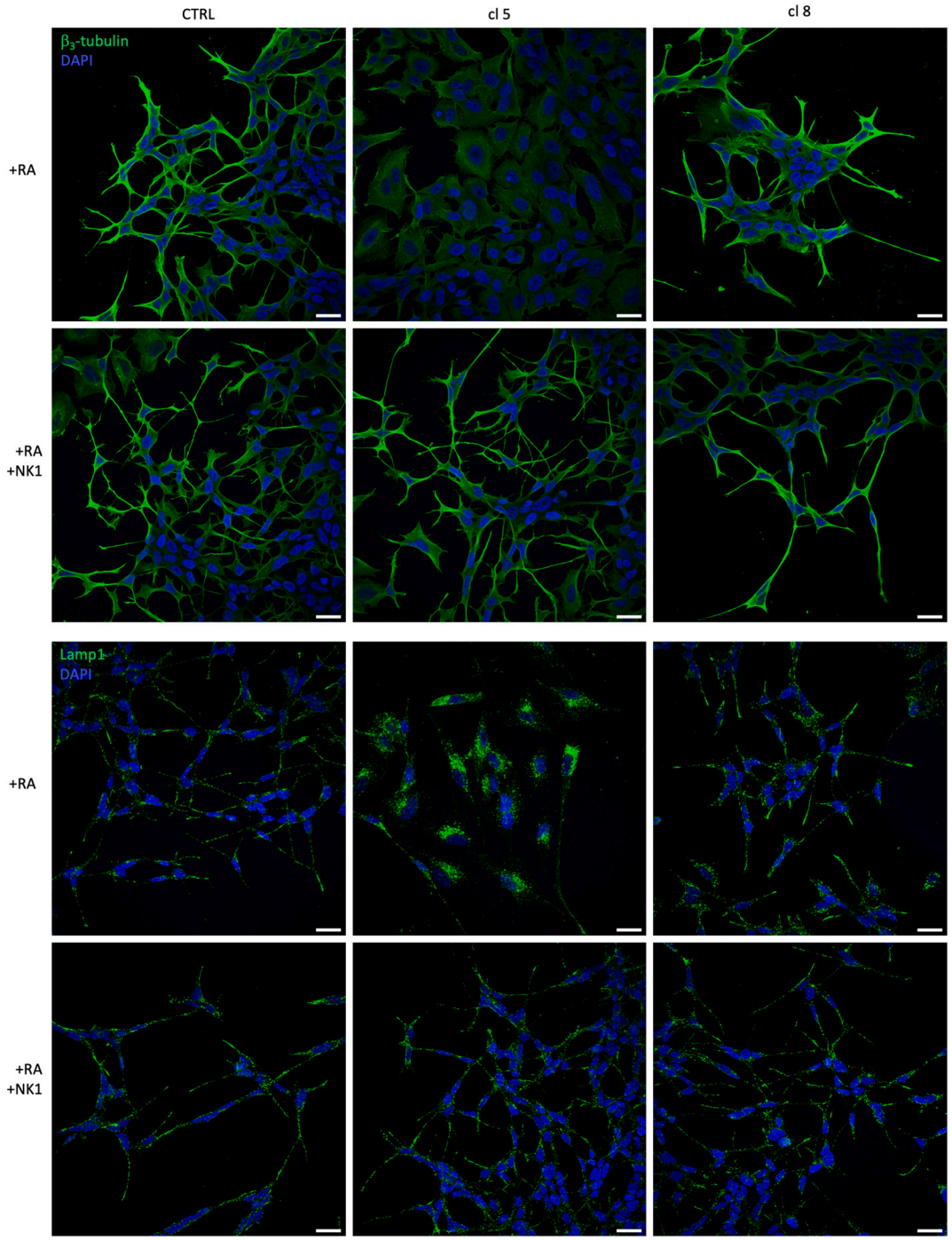

Fig. 6. NK1 treatment stimulates neuronal differentiation of the NAGLU silenced clones. Neuronal differentiation of SK-NBE CTRL clone and NAGLU silenced stable clones (cl5 and cl 8) were handled as described in Fig. 5. Neuronal differentiation success was followed by confocal microscopy using a specific antibody against β_3-Tubulin. Lysosome distribution was analyzed by using a specific antibody against Lamp1 (marker of the lysosomal compartment). Nuclei were decorated by DAPI staining. Single focal sections are shown. Scale bar: 50 μm.

growth factor/receptor binding and downstream signaling [20]. In human-induced pluripotent stem cells (iPSC) derived from the skin fibroblasts of children affected by MPS IIIB, the excess of HS interferes with FGF signaling leading to the impairment of iPSC differentiation [41]. In the mouse model of the MPS IIIB, extracellular HS accumulation is associated with reduced levels of FGF receptor (FGFR) and FGF2 mRNA resulting in the inhibition of neurogenesis and attenuated plasticity of astrocytes [42]. Moreover, HS build-up affects integrin-mediated focal adhesion assembly/disassembly in MPS IIIB mouse astrocytes and human neuronal progenitor cells, leading to defects of cell polarization and migration [14]. In line with these data, we recently found that the excess of extracellular HS sequesters FGF2, thus impairing the activation of FGFR/FGF2 signaling in cultured fibroblasts from MPS I and IIIB patients [7]. Interestingly, we demonstrated that the recombinant NK1 protein can reverse deregulated cell signaling such as FGF-dependent ERK1/2 phosphorylation in MPS I and MPS IIIB fibroblasts. We also showed that NK1 reduces lysosomal HS storage in these cellular models of the disease [7]. In this study, we demonstrate that NK1 reduces the lysosomal pathology in a model of neuronal cells lacking NAGLU that reproduces the MPS IIIB phenotype, showing an

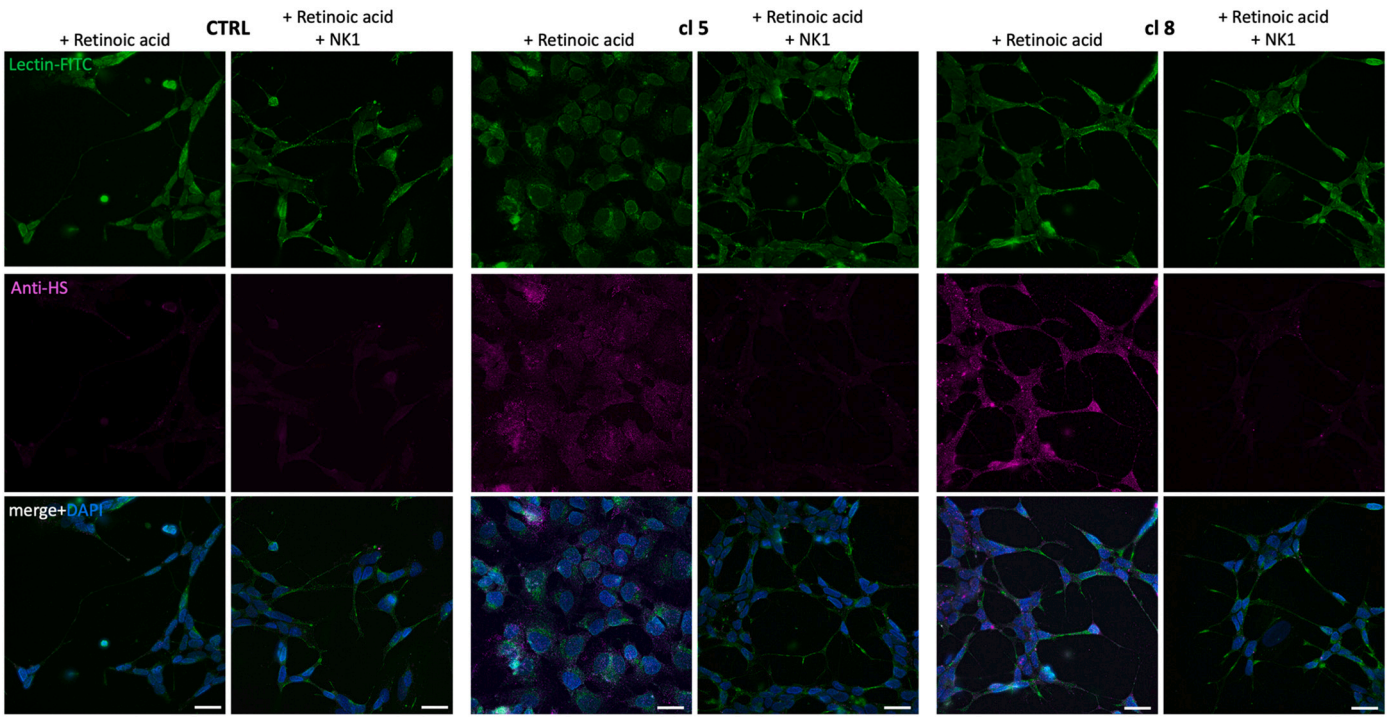

Fig. 7. Effect of NK1 treatment on HS accumulation during neuronal differentiation of NAGLU silenced clones. SK-NBE CTRL clone and NAGLU silenced stable clones (cl5 and cl 8) were differentiated as described in Fig. 5, in the presence or absence of NK1. The GAGs/HS distribution was analyzed by fluorescence microscopy by using the anti-HS antibody 10E4 and Lectin-FITC probe, respectively. Nuclei were decorated by DAPI staining. Single focal sections are shown. Scale bar: 50 μm.

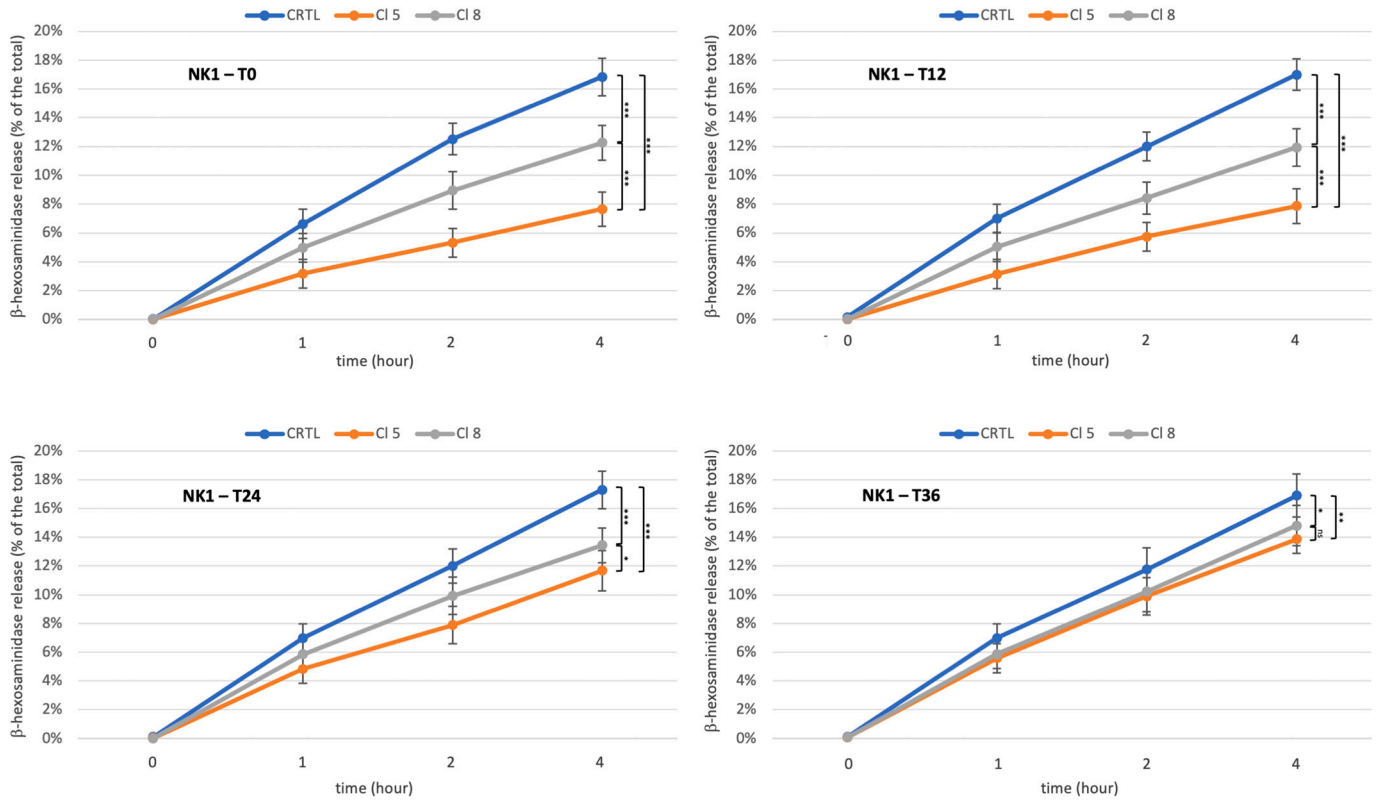

Fig. 8. Effect of NK1 treatment on lysosomal secretion in NAGLU silenced stable clones. SK-NBE CTRL clone and NAGLU silenced stable clones (cl 5 and cl 8) were treated for 36 h with NK1, and lysosomal secretion was measured over time by means of β-hexosaminidase release assay. β-hexosaminidase released from the SK-NBE clones was measured over time up to 4 h in the absence or presence of NK1. Mean-values were obtained by three independent experiments. Asterisks indicate the statistically significant differences: (***) p-value < 0.0001, (**) p-value < 0.001, (*) p-value < 0.005.

impressive accumulation of HS in both lysosomes and cell membrane. Furthermore, we show that NK1 treatment stimulates the differentiation of NAGLU silenced SK-NBE into neuron-like cells, thus suggesting that NK1 can reactivate cell signaling involved in the neuronal differentiation process. Although further investigations on the molecular mechanisms of action of NK1 are needed, here we demonstrate that NK1 treatment reduces GAG/HS accumulation in our MPS IIIB cellular model by restoring the physiological lysosome exocytosis.

Overall, our findings might be relevant for the development of new therapeutic strategies for the cure of MPS IIIB as well as of other MPS types and lysosomal storage diseases characterized by severe neurological phenotypes.

4. Materials and methods

4.1. Chemicals

Dulbecco Modified Eagle's Medium (DMEM), RPMI-1640, fetal bovine serum (FBS), penicillin, streptomycin, and phosphate-buffered saline (PBS) from Gibco, Thermo Fisher Scientific (Carlsbad, CA, USA); ECL System from Amersham Pharmacia (Buckinghamshire, UK); Bradford assay reagents from Bio-Rad (München, Germany); bovine serum albumin (BSA) (10711454001) and protease inhibitor cocktail tablets (04693132001) from Roche Diagnostics (Grenoble, France); formaldehyde solution 37% (F15587), methanol (34860), trizma base (1503), glycine (G8898), acrylamide/bis-acrylamide 30% solution (A3699), Lectin from Triticum vulgaris (wheat) FITC conjugate (L4895), 4-methylumbelliferyl-*N*-acetyl-α-D-glucosaminide (474500) from Sigma-Aldrich (St. Louis, MI, USA); ProLong™ Gold Antifade Mountant with DAPI (P36935) and LysoTracker (L7528) from Thermo Fisher Scientific (Carlsbad, CA, USA), IBAfect reagent (7-2005-050) from IBA Lifesciences (Goettingen, Germany).

4.2. Antibodies

The following antibodies were used: for immunofluorescence analyses, mouse monoclonal anti-CD107a (anti-Lamp1) (SAB4700416 clone H4A3) from Sigma-Aldrich (St. Louis, MI, USA), rabbit polyclonal anti-Calnexin (SPC-108) from StressMarq Biosciences Inc. (Victoria, Canada), rabbit polyclonal ant-GM130 (#12480) from Cell Signaling Technology (Danvers, MA, USA), mouse and rabbit Alexa-Fluor (488 and 546) secondary antibodies A11029, A11030, A11034, and A11035, were from Thermo Fisher Scientific-Invitrogen, (Carlsbad, CA, USA). For Western blot analyses, rabbit anti-NAGLU monoclonal antibody (ab214671) from Abcam (Cambridge, MA, USA), mouse anti-β-actin monoclonal antibody (G043) from Abm (Richmond, Canada), secondary antibodies were goat anti-mouse IgG polyclonal antibody conjugated to horseradish peroxidase (HRP) (sc-2031) and goat anti-rabbit IgG-HRP polyclonal antibody (sc-3837) from Santa Cruz Biotechnology (Heidelberg, Germany).

4.3. Cell culture and transfection

SK-NBE human neuroblastoma cell line (CRL-2271 ATCC, Wesel, Germany) was cultured in RPMI-1640, 2 mM L-glutamine, 1 mM sodium pyruvate, supplemented with 10% FBS, 100 units/ml penicillin, and 100 μg/ml streptomycin, at 37 °C in a humidified 5% CO_2 atmosphere. For stable transfections, SK-NBE were plated at a density of 5×10^5 cells/100-mm tissue culture dish in antibiotic-free RPMI-1640 containing 10% FBS and incubated for 24 h at 37 °C with 5% CO_2. In total, 60–70% confluent cells were transfected using IBAfect reagent, according to the manufacturer's instructions, with a pool of plasmids codifying for three shRNAs (188A12, 566F3, and 526A3) targeting NAGLU or with a control plasmid codifying for a non-targeting shRNA (Open Biosystems, Lafayette, CO, USA). Forty-eight hours later, transfected SK-NBE were selected in the presence of 0.7 μg/ml of puromycin and subjected to enzymatic activity assay to identify the stable NAGLU-silenced clones. Stable clones were grown in the same culture medium of the SK-NBE supplemented with 0.7 μg/ml of puromycin for all the experimentation.

Fibroblasts from MPS-affected patients were kindly provided by the Cell Line and DNA Biobank from Patients Affected by Genetic Diseases (Istituto G. Gaslini, Genoa, Italy) [43]. Primary Human Dermal Fibroblasts, adult (HDFa, from Thermo Fisher Scientific), and MPS fibroblasts were cultured in DMEM, supplemented with 10% FBS, 2 mM L-glutamine, 100 U/ml penicillin, and 100 mg/ml streptomycin, at 37 °C in a humidified 5% CO_2 atmosphere.

4.4. Enzyme activity assay

To determine NAGLU enzymatic activity in stable clones, pellets from 5×10^5 cells of each clone were collected, submitted to 10 freeze-thaw cycles, and clarified by centrifugation. Protein concentration of the samples was determined by the Lowry method. NAGLU enzymatic activity of each clone was measured as described by Marsh and Fensom using 4-methylumbelliferyl-*N*-acetyl-α-D-glucosaminide as fluorogenic substrate [6,44]. Enzymatic activity was normalized for total protein concentration, and hydrolysis of 1 nmol of substrate per hour per milligram of protein was defined as one catalytic unit.

4.5. Fluorescence microscopy

Immunofluorescence staining was performed as previously reported [45–47]. Briefly, cells grown on glass coverslips were washed with PBS and fixed in 3.7% formaldehyde at room temperature for 30 min. After fixation, cells were washed with PBS and permeabilized by incubation in blocking buffer (PBS containing 1% BSA, 0.01% sodium azide, and 0.02% Saponin) for 10 min at room temperature. Cells were then incubated with the indicated primary antibodies diluted in the same blocking buffer for 1 h at room temperature. Cells were washed three times with PBS and incubated with the corresponding secondary antibodies for 30 min at room temperature. Finally, coverslips were washed in distilled water and mounted onto glass slides with the Prolong Gold anti-fade reagent with DAPI. Images were collected using a laser-scanning microscope (LSM 700, Carl Zeiss Microimaging, Inc., Jena, Germany) equipped with a planapo 63× oil immersion (NA 1.4) objective lens.

4.6. Western blotting

Cells, grown to sub-confluence in standard medium, were harvested in lysis buffer (50 mM Tris pH 7.5, 150 mM NaCl, 1 mM EDTA, 1 mM EGTA, 10% glycerol, 1% Triton X-100, 1 mM β-glycerophosphate, 1 mM phenylmethylsulfonyl fluoride, protease inhibitor cocktail tablet, 1 mM sodium orthovanadate, and 2.5 mM sodium pyrophosphate) [48]. The lysates were incubated for 30 min on ice, and supernatants were collected and centrifuged for 30 min at 14,000 ×*g*. Protein concentration was estimated by Bradford assay, and 25 or 50 μg/lane of total proteins were separated on SDS gels and transferred to nitrocellulose membranes. Membranes were treated with a blocking buffer (25 mM Tris, pH 7.4, 200 mM NaCl, 0.5% Triton X-100) containing 5% non-fat powdered milk for 1 h at room temperature. Incubation with the primary antibody was carried out overnight at 4 °C. After washings, membranes were incubated with the HRP-conjugated secondary antibody for 1 h at room temperature. Following further washings of the membranes, chemiluminescence was generated by enhanced chemiluminescence (ECL) kit.

4.7. β-Hexosaminidase release assay

Confluent monolayers of cells were grown in 6-well plates for 24 h before being subjected to enzymatic activity measurement in the

extracellular *vs* the intracellular extracts. On the day of the assay, the media were replaced by Optimem and left to incubate for 4 h. 50 ml of the extracellular media were picked up every hour and transferred in a black 96-well plate on ice. After 4 h, cells were lysed in 500 μl of lysis buffer (50 mM HEPES, 150 mM NaCl, 1 mM EDTA, 1 mM EGTA, 10% glycerol, and 1% Triton-X-100) supplemented with protease and phosphatase inhibitors. For each experimental point, 50 μl of every sample was incubated for 30 min at 37 C with 10 μl of 6 mM 4-methyl-umbellyferyl-*N*-acetyl-β-D-glucosaminide in sodium citrate-phosphate buffer, pH 4.5. The reaction was stopped by adding 40 μl of 2 M Na2CO3 and 1.1 M glycine, and the fluorescence was measured at excitation 365 nm/emission 450 nm. The β-hexosaminidase release was measured and shown as a percentage of the extracellular *versus* the intracellular enzymatic activity.

4.8. Statistical analysis

Data reported are expressed as the mean ± SD of at least three separate experiments. Statistical significance was determined by Student's *t*-test and ONE-WAY ANOVA test.

Supplementary data to this article can be found online at https://doi.org/10.1016/j.bbamcr.2021.119113.

CRediT authorship contribution statement

V.D.P., M.D.A., and L.M.P. conceived the study. V.D.P., G.S., M.S., and M.D.A. designed and carried out the experiments and analyzed the data. VDP., M.D.A., and L.M.P. wrote the manuscript with input from all the other authors. All authors approved the manuscript.

Declaration of competing interest

Luigi Michele Pavone has licensed compositions comprising hepatocyte growth factor or variants thereof for use in the treatment of mucopolysaccharidoses (granted Italian patent MI2014A001454). The authors declare no additional competing financial interests.

Acknowledgments

This work was supported by funds from the Cure Sanfilippo Foundation USA grant “Targeting Heparan Sulfate Proteoglycans as a Novel Therapeutic Strategy for Sanfilippo diseases” 2021–2024 to L.M.P. The Cell Line and DNA Biobank from Patients Affected by Genetic Diseases (Istituto G. Gaslini), member of the Telethon Network of Genetic Biobanks (project GTB12001), funded by Telethon Italy, provided us with specimens (fibroblasts from MPS patients).

References

[1] E.F. Neufeld, J. Muenzer, The Mucopolysaccharidoses, McGraw-Hill, New York, 2001.
[2] J. Zhou, J. Lin, W.T. Leung, L. Wang, A basic understanding of mucopolysaccharidosis: incidence, clinical features, diagnosis, and management, Intractable Rare Dis. Res. 9 (2020) 1–9, https://doi.org/10.5582/irdr.2020.01011.
[3] A. Fedele, Sanfilippo syndrome: causes, consequences, and treatments, Appl. Clin. Genet. (2015) 269, https://doi.org/10.2147/TACG.S57672.
[4] N. Benetó, L. Vilageliu, D. Grinberg, I. Canals, Sanfilippo syndrome: molecular basis, disease models and therapeutic approaches, Int. J. Mol. Sci. 21 (2020) 7819, https://doi.org/10.3390/ijms21217819.
[5] G.G. Schiattarella, G. Cerulo, V. De Pasquale, P. Cocchiaro, O. Paciello, L. Avallone, M.P. Belfiore, F. Iacobellis, D. Di Napoli, F. Magliulo, C. Perrino, B. Trimarco, G. Esposito, P. Di Natale, L.M. Pavone, The murine model of mucopolysaccharidosis IIIB develops cardiopathies over time leading to heart failure, PLoS One 10 (2015), https://doi.org/10.1371/journal.pone.0131662.
[6] V. De Pasquale, A. Pezone, P. Sarogni, A. Tramontano, G.G. Schiattarella, V. E. Avvedimento, S. Paladino, L.M. Pavone, EGFR activation triggers cellular hypertrophy and lysosomal disease in NAGLU-depleted cardiomyoblasts, mimicking the hallmarks of mucopolysaccharidosis IIIB, Cell Death Dis. 9 (2018), https://doi.org/10.1038/s41419-017-0187-0.
[7] V. De Pasquale, P. Sarogni, V. Pistorio, G. Cerulo, S. Paladino, L.M. Pavone, Targeting Heparan sulfate proteoglycans as a novel therapeutic strategy for mucopolysaccharidoses, Mol. Ther. Methods Clin. Dev. 10 (2018), https://doi.org/10.1016/j.omtm.2018.05.002.
[8] V. De Pasquale, M. Caterino, M. Costanzo, R. Fedele, M. Ruoppolo, L.M. Pavone, Targeted metabolomic analysis of a mucopolysaccharidosis IIIB mouse model reveals an imbalance of branched-chain amino acid and fatty acid metabolism, Int. J. Mol. Sci. 21 (2020) 4211, https://doi.org/10.3390/ijms21124211.
[9] M.P. Belfiore, F. Iacobellis, E. Acampora, M. Caiazza, M. Rubino, E. Monda, M. R. Magaldi, A. Tarallo, M. Sasso, V. De Pasquale, R. Grassi, S. Cappabianca, P. Calabrò, S. Fecarotta, S. Esposito, G. Esposito, A. Pisani, L.M. Pavone, G. Parenti, G. Limongelli, Aortopathies in mouse models of pompe, fabry and mucopolysaccharidosis IIIB lysosomal storage diseases, PLoS One 15 (2020), e0233050, https://doi.org/10.1371/journal.pone.0233050.
[10] V. De Pasquale, M. Costanzo, R.A. Siciliano, M.F. Mazzeo, V. Pistorio, L. Bianchi, E. Marchese, M. Ruoppolo, L.M. Pavone, M. Caterino, Proteomic analysis of mucopolysaccharidosis IIIB mouse brain, Biomolecules (2020), https://doi.org/10.3390/biom10030355.
[11] C. Pan, M.S. Nelson, M. Reyes, L. Koodie, J.J. Brazil, E.J. Stephenson, R.C. Zhao, C. Peters, S.B. Selleck, S.E. Stringer, P. Gupta, Functional abnormalities of heparan sulfate in mucopolysaccharidosis-I are associated with defective biologic activity of FGF-2 on human multipotent progenitor cells, Blood. 106 (2005) 1956–1964, https://doi.org/10.1182/blood-2005-02-0657.
[12] R.J. Holley, A. Deligny, W. Wei, H.A. Watson, M.R. Niñonuevo, A. Dagälv, J. A. Leary, B.W. Bigger, L. Kjellén, C.L.R. Merry, I. Mucopolysaccharidosis Type, Unique structure of accumulated heparan sulfate and increased N-sulfotransferase activity in mice lacking α-l-iduronidase, J. Biol. Chem. 286 (2011) 37515–37524, https://doi.org/10.1074/jbc.M111.287474.
[13] D.M. McCarty, J. DiRosario, K. Gulaid, S. Killedar, A. Oosterhof, T.H. van Kuppevelt, P.T. Martin, H. Fu, Differential distribution of heparan sulfate glycoforms and elevated expression of heparan sulfate biosynthetic enzyme genes in the brain of mucopolysaccharidosis IIIB mice, Metab. Brain Dis. 26 (2011) 9–19, https://doi.org/10.1007/s11011-010-9230-x.
[14] J. Bruyère, E. Roy, J. Ausseil, T. Lemonnier, G. Teyre, D. Bohl, S. Etienne-Manneville, H. Lortat-Jacob, J.M. Heard, S. Vitry, Heparan sulfate saccharides modify focal adhesions: implication in mucopolysaccharidosis neuropathophysiology, J. Mol. Biol. 427 (2015) 775–791, https://doi.org/10.1016/j.jmb.2014.09.012.
[15] J.M. Heppner, F. Zaucke, L.A. Clarke, Extracellular matrix disruption is an early event in the pathogenesis of skeletal disease in mucopolysaccharidosis I, Mol. Genet. Metab. 114 (2015) 146–155, https://doi.org/10.1016/j.ymgme.2014.09.012.
[16] S.D.K. Kingma, T. Wagemans, L. IJlst, A.L.J.J. Bronckers, T.H. van Kuppevelt, V. Everts, F.A. Wijburg, N. van Vlies, Altered interaction and distribution of glycosaminoglycans and growth factors in mucopolysaccharidosis type I bone disease, Bone. 88 (2016) 92–100, https://doi.org/10.1016/j.bone.2016.01.029.
[17] R. Costa, A. Urbani, M. Salvalaio, S. Bellesso, D. Cieri, I. Zancan, M. Filocamo, P. Bonaldo, I. Szabò, R. Tomanin, E. Moro, Perturbations in cell signaling elicit early cardiac defects in mucopolysaccharidosis type II, Hum. Mol. Genet. 26 (2017) 1643–1655, https://doi.org/10.1093/hmg/ddx069.
[18] C.A. Dwyer, S.L. Scudder, Y. Lin, L.E. Dozier, D. Phan, N.J. Allen, G.N. Patrick, J. D. Esko, Neurodevelopmental changes in excitatory synaptic structure and function in the cerebral cortex of Sanfilippo syndrome IIIA mice, Sci. Rep. 7 (2017) 46576, https://doi.org/10.1038/srep46576.
[19] B.W. Bigger, D.J. Begley, D. Virgintino, A.V. Pshezhetsky, Anatomical changes and pathophysiology of the brain in mucopolysaccharidosis disorders, Mol. Genet. Metab. 125 (2018) 322–331, https://doi.org/10.1016/j.ymgme.2018.08.003.
[20] V. De Pasquale, L.M. Pavone, Heparan sulfate proteoglycans: the sweet side of development turns sour in mucopolysaccharidoses, Biochim. Biophys. Acta Mol. Basis Dis. 1865 (2019), 165539, https://doi.org/10.1016/j.bbadis.2019.165539.
[21] P.C. Billings, M. Pacifici, Interactions of signaling proteins, growth factors and other proteins with heparan sulfate: mechanisms and mysteries, Connect. Tissue Res. 56 (2015) 272–280, https://doi.org/10.3109/03008207.2015.1045066.
[22] E.N. Barnes, J.L. Biedler, B.A. Spengler, K.M. Lyser, The fine structure of continuous human neuroblastoma lines SK-N-SH, SK-N-BE(2), and SK-N-MC, In Vitro 17 (1981) 619–631, https://doi.org/10.1007/BF02618461.
[23] N. Sidell, A. Altman, M.R. Haussler, R.C. Seeger, Effects of retinoic acid (RA) on the growth and phenotypic expression of several human neuroblastoma cell lines, Exp. Cell Res. 148 (1983) 21–30, https://doi.org/10.1016/0014-4827(83)90184-2.
[24] C.G. Leotta, C. Federico, M.V. Brundo, S. Tosi, S. Saccone, HLXB9 gene expression, and nuclear location during in vitro neuronal differentiation in the SK-N-BE neuroblastoma cell line, PLoS One 9 (2014), e105481, https://doi.org/10.1371/journal.pone.0105481.
[25] S. Bellesso, M. Salvalaio, S. Lualdi, E. Tognon, R. Costa, P. Braghetta, C. Giraudo, R. Stramare, L. Rigon, M. Filocamo, R. Tomanin, E. Moro, FGF signaling deregulation is associated with early developmental skeletal defects in animal models for mucopolysaccharidosis type II (MPSII), Hum. Mol. Genet. 27 (2018) 2262–2275, https://doi.org/10.1093/hmg/ddy131.
[26] H.A. Watson, R.J. Holley, K.J. Langford-Smith, F.L. Wilkinson, T.H. van Kuppevelt, R.F. Wynn, J.E. Wraith, C.L.R. Merry, B.W. Bigger, Heparan sulfate inhibits hematopoietic stem and progenitor cell migration and engraftment in mucopolysaccharidosis I, J. Biol. Chem. 289 (2014) 36194–36203, https://doi.org/10.1074/jbc.M114.599944.
[27] G. David, X.M. Bai, B. Van der Schueren, J.J. Cassiman, H. Van den Berghe, Developmental changes in heparan sulfate expression: in situ detection with mAbs, J. Cell Biol. 119 (1992) 961–975, https://doi.org/10.1083/jcb.119.4.961.
[28] J. van den Born, K. Salmivirta, T. Henttinen, N. Östman, T. Ishimaru, S. Miyaura, K. Yoshida, M. Salmivirta, Novel heparan sulfate structures revealed by

monoclonal antibodies, J. Biol. Chem. 280 (2005) 20516–20523, https://doi.org/10.1074/jbc.M502065200.
[29] C. Martins, H. Hůlková, L. Dridi, V. Dormoy-Raclet, L. Grigoryeva, Y. Choi, A. Langford-Smith, F.L. Wilkinson, K. Ohmi, G. DiCristo, E. Hamel, J. Ausseil, D. Cheillan, A. Moreau, E. Svobodová, Z. Hájková, M. Tesařová, H. Hansíková, B. W. Bigger, M. Hrebícek, A.V. Pshezhetsky, Neuroinflammation, mitochondrial defects and neurodegeneration in mucopolysaccharidosis III type C mouse model, Brain. 138 (2015) 336–355, https://doi.org/10.1093/brain/awu355.
[30] S. Gustavsson, E. Ohlin Sjöström, A. Tjernberg, J. Janson, U. Westermark, T. Andersson, Å. Makower, E. Arnelöf, G. Andersson, J. Svartengren, C. Ekholm, S. Svensson Gelius, Intravenous delivery of a chemically modified sulfamidase efficiently reduces heparan sulfate storage and brain pathology in mucopolysaccharidosis IIIA mice, Mol. Genet. Metab. Rep. 21 (2019), 100510, https://doi.org/10.1016/j.ymgmr.2019.100510.
[31] B. Chazotte, Labeling membrane glycoproteins or glycolipids with fluorescent wheat germ agglutinin, Cold Spring Harb. Protoc. (2011) (2011), https://doi.org/10.1101/pdb.prot5623 pdb.prot5623-pdb.prot5623.
[32] J.C. Roney, S. Li, T. Farfel-Becker, N. Huang, T. Sun, Y. Xie, X.-T. Cheng, M.-Y. Lin, F.M. Platt, Z.-H. Sheng, Lipid-mediated motor-adaptor sequestration impairs axonal lysosome delivery leading to autophagic stress and dystrophy in Niemann-Pick type C, Dev. Cell 56 (2021) 1452–1468.e8, https://doi.org/10.1016/j.devcel.2021.03.032.
[33] G. Scerra, V. De Pasquale, L.M. Pavone, M.G. Caporaso, A. Mayer, M. Renna, M. D'Agostino, Early onset effects of single substrate accumulation recapitulate major features of LSDs-patients derived lysosomes, IScience (2021), 102707, https://doi.org/10.1016/j.isci.2021.102707.
[34] A. Fraldi, A.D. Klein, D.L. Medina, C. Settembre, Brain disorders due to lysosomal dysfunction, Annu. Rev. Neurosci. 39 (2016) 277–295, https://doi.org/10.1146/annurev-neuro-070815-014031.
[35] M. Scarpa, P.J. Orchard, A. Schulz, P.I. Dickson, M.E. Haskins, M.L. Escolar, R. Giugliani, Treatment of brain disease in the mucopolysaccharidoses, Mol. Genet. Metab. 122 (2017) 25–34, https://doi.org/10.1016/j.ymgme.2017.10.007.
[36] R. Heon-Roberts, A.L.A. Nguyen, A.V. Pshezhetsky, Molecular bases of neurodegeneration and cognitive decline, the major burden of Sanfilippo disease, J. Clin. Med. 9 (2020) 344, https://doi.org/10.3390/jcm9020344.
[37] L. Gaffke, K. Pierzynowska, E. Piotrowska, G. Węgrzyn, How close are we to therapies for Sanfilippo disease? Metab. Brain Dis. 33 (2018) 1–10, https://doi.org/10.1007/s11011-017-0111-4.
[38] Y. Pearse, M. Iacovino, A cure for Sanfilippo syndrome? A summary of current therapeutic approaches and their promise, Med. Res. Arch. 8 (2020), https://doi.org/10.18103/mra.v8i2.2045.
[39] A.V. Pshezhetsky, Lysosomal storage of heparan sulfate causes mitochondrial defects, altered autophagy, and neuronal death in the mouse model of mucopolysaccharidosis III type C, Autophagy. 12 (2016) 1059–1060, https://doi.org/10.1080/15548627.2015.1046671.
[40] S. Fecarotta, A. Tarallo, C. Damiano, N. Minopoli, G. Parenti, Pathogenesis of mucopolysaccharidoses, an update, Int. J. Mol. Sci. (2020), https://doi.org/10.3390/ijms21072515.
[41] T. Lemonnier, S. Blanchard, D. Toli, E. Roy, S. Bigou, R. Froissart, I. Rouvet, S. Vitry, J.M. Heard, D. Bohl, Modeling neuronal defects associated with a lysosomal disorder using patient-derived induced pluripotent stem cells, Hum. Mol. Genet. 20 (2011) 3653–3666, https://doi.org/10.1093/hmg/ddr285.
[42] H.H. Li, H.-Z. Zhao, E.F. Neufeld, Y. Cai, F. Gómez-Pinilla, Attenuated plasticity in neurons and astrocytes in the mouse model of Sanfilippo syndrome type B, J. Neurosci. Res. 69 (2002) 30–38, https://doi.org/10.1002/jnr.10278.
[43] M. Filocamo, R. Mazzotti, F. Corsolini, M. Stroppiano, G. Stroppiana, S. Grossi, S. Lualdi, B. Tappino, F. Lanza, S. Galotto, R. Biancheri, Cell line and DNA biobank from patients affected by genetic diseases, Open J. Bioresour. 1 (2014), e2, https://doi.org/10.5334/ojb.ab.
[44] J. Marsh, A.H. Fensom, 4-Methylumbelliferyl α-N-acetylglucosaminidase activity for diagnosis of Sanfilippo B disease, Clin. Genet. 27 (2008) 258–262, https://doi.org/10.1111/j.1399-0004.1985.tb00217.x.
[45] M. Ciano, S. Allocca, M.C. Ciardulli, L. della Volpe, S. Bonatti, M. D'Agostino, Differential phosphorylation-based regulation of αB-crystallin chaperone activity for multipass transmembrane proteins, Biochem. Biophys. Res. Commun. 479 (2016) 325–330, https://doi.org/10.1016/j.bbrc.2016.09.071.
[46] M. D'Agostino, G. Scerra, M. Cannata Serio, M.G. Caporaso, S. Bonatti, M. Renna, Unconventional secretion of α-Crystallin B requires the autophagic pathway and is controlled by phosphorylation of its serine 59 residue, Sci. Rep. 9 (2019) 16892, https://doi.org/10.1038/s41598-019-53226-x.
[47] C. Caiazza, M. D'Agostino, F. Passaro, D. Faicchia, M. Mallardo, S. Paladino, G. M. Pierantoni, D. Tramontano, Effects of long-term citrate treatment in the PC3 prostate cancer cell line, Int. J. Mol. Sci. 20 (2019) 2613, https://doi.org/10.3390/ijms20112613.
[48] G. Cerulo, S. Tafuri, V. De Pasquale, S. Rea, S. Romano, A. Costagliola, R. Della Morte, L. Avallone, L.M. Pavone, Serotonin activates cell survival and apoptotic death responses in cultured epithelial thyroid cells, Biochimie. 105 (2014), https://doi.org/10.1016/j.biochi.2014.06.020.